ACS OMEGA

http://pubs.acs.org/journal/acsodf

Article

An Electronic and Optically Controlled Bifunctional Transistor Based on a Bio−Nano Hybrid Complex

Vikram Bakaraju, E. Senthil Prasad, Brijesh Meena, and Harsh Chaturvedi*

Cite This: *ACS Omega* 2020, 5, 9702−9706

Read Online

ACCESS | Metrics & More | Article Recommendations

ABSTRACT: We report an electronically and optically controlled bioelectronic field-effect transistor (FET) based on the hybrid film of photoactive bacteriorhodopsin and electronically conducting single-walled carbon nanotubes (SWNTs). Two-dimensional (2D) crystals of bacteriorhodopsin form the photoactive center of the bio−nano complex, whereas one-dimensional (1D) pure SWNTs provide the required electronic support. The redshift in the Raman spectra indicates the electronic doping with an estimated charge density of 3×10^6 cm^{-2}. The hybrid structure shows a conductivity of 19 μS/m and semiconducting characteristics due to preferential binding with selective diameters of semiconducting SWNTs. The bioelectronic transistor fabricated using direct laser lithography shows both optical and electronic gating with a significant on/off switch ratio of 8.5 and a photoconductivity of 13.15 μS/m. An n-type FET shows complementary p-type characteristics under light due to optically controlled, electronic doping by the "proton-pumping" bacteriorhodopsin. The fabricated bioelectronic transistor exhibits both electronically and optically well-controlled bifunctionality based on the functionalized hybrid electronic material.

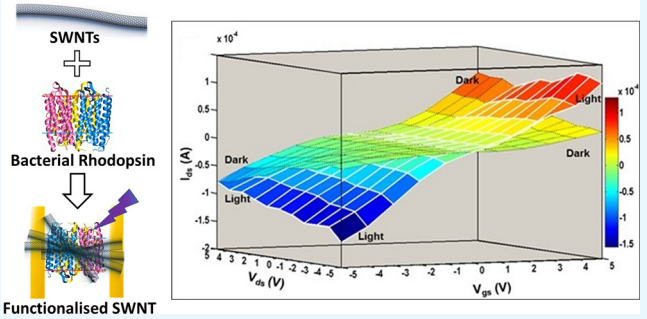

INTRODUCTION

Bioelectronics aims to use electronic/optically active, functional biological molecules (chromophores, proteins, etc.) as an active material for electronic or photonic devices. Research on bio−nano hybrid materials is being actively pursued for potential application in developing functional, electro-optical devices and biological sensors.[1−3] Donor−acceptor systems, based on SWNTs functionalized with inorganic or organic polymers,[4] biological DNA,[5−7] protein, etc., have been widely reported in pursuit of fabricating such hybrid devices.[8] Devices such as field-effect transistors, sensors, and rectifiers based on SWNTs functionalized with optically active materials like quantum dots, inorganic ruthenium dyes, or optically active molecules have been fabricated.[9] Photoactive proteins/molecules can bind either covalently or noncovalently with SWNTs to form a stable donor−acceptor system.[10,11] However, noncovalent functionalization of SWNTs is generally preferred for electro-optical devices as it preserves the electronic nature of SWNTs in the functionalized hybrid complex.

Diverse devices are being proposed, based on SWNTs functionalized with optically active, biological molecules.[12,13] Bacteriorhodopsin (bR) is a stable optically active protein, widely proposed for its technological application in developing various electronic and photonic devices such as optical data storage, electro-optical memory, logic gates, and photochromatic and holographic systems. Recent reports of functionalization of bacteriorhodopsin with nanoparticles (quantum dots, nanotubes) show an active interest in using a functionalized bio−nano hybrid complex for developing novel photovoltaic, electro-optical devices.[14,15] Herein, we report the fabrication of electronic and optically bifunctional field-effect transistor (FET) based on SWNTs functionalized with bacteriorhodopsin. The fabricated bioelectronic transistor shows intrinsically semiconducting electro-optical properties with well-controlled electronic and optical gating, optical doping, and photoconductivity.

Bacteriorhodopsin forms the optical center of the purple membrane (PM). The purple membrane is made up of 75% proteins and 25% lipids.[16] The only protein present in the purple membrane is the bacteriorhodopsin, which acts as a light-driven proton pump.[16] The photocycle of bacteriorhodopsin in the purple membrane has been well characterized and duly reported. The PM remains stable up to 80 °C and has a buoyant density of 1.18 g/cm^3 and a refractive index of 1.45−1.55, and its natural stable crystalline structure makes the

Received: November 15, 2019
Accepted: March 19, 2020
Published: April 20, 2020

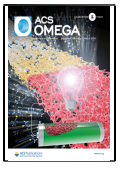

https://dx.doi.org/10.1021/acsomega.9b03904
ACS Omega 2020, 5, 9702−9706

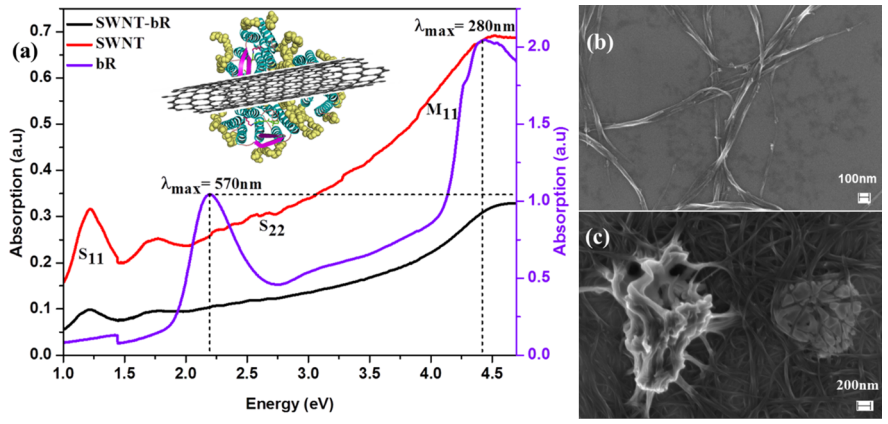

Figure 1. . (a) Absorption spectra of pure SWNT (red) and bacteriorhodopsin (bR) (purple) control solutions and that of the functionalized SWNT−bR complex. SEM images of (b) pure SWNT and (c) SWNT functionalized with bR complex.

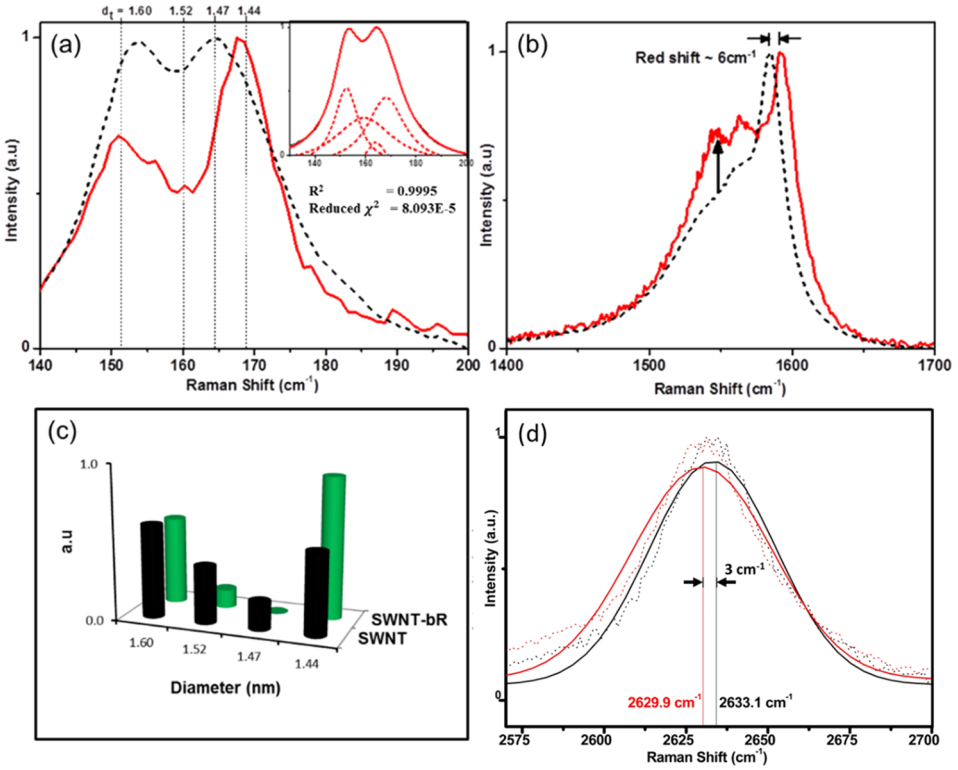

Figure 2. Raman spectra showing (a) RBM (radial breathing mode) of SWNTs (black) and the functionalized complex of SWNT−bR (red) showing stable preferential binding with specific diameters. (b) G band showing changes in G^+ (1591 cm^{-1}) and G^- (1540 cm^{-1}) peaks of the SWNT−bR complex as compared to pure SWNTs. (c) Histogram showing preferential binding with the enrichment of SWNTs of specific diameters. (d) G′ band showing a slight redshift (3 cm^{-1}).

purple membrane an excellent two-dimensional (2D) optical material for the development of bioelectronics.[17,18] Optoelectronic and photonic applications demand a high quantity (several milligrams) of thin films of the purple membrane. For large-scale incubation of bacteriorhodopsin, Halobacterium cultivation was performed in a 7 L photobioreactor. The purified purple membrane was characterized using a UV−vis spectrophotometer by taking the ratio of absorptions at 280 and 560 nm. Along with a high yield of 14.4 mg/L, the extracted PM shows high quality with a ratio estimated using absorption peaks to be around ∼2.0 to 2.1. In Figure 1, 2 mg/mL of this extracted protein aliquot was used for further functionalization with SWNTs.

The proposed bio−nano devices based on SWNTs are limited due to the inherent hydrophobic nature of pristine SWNTs. However, aqueous solutions of SWNTs have been reported using surfactants.[19] Herein, biocompatible phospholipid polyethylene glycol amine was used as the surfactant to prepare a well-dispersed aqueous solution of pure SWNTs.[20]

RESULTS AND DISCUSSION

Ultrapure (99.5%) SWNTs, purchased from NanoIntegris in the form of sheets (batch number: P10-126) were dispersed in water using 1,2-distearoyl-*sn*-glycero-3-phosphoethanolamine-*N*-amino [(polyethylene Glycol) 2000] (ammonium salt) (product code: 880128P), bought from Sigma-Aldrich. Well-

https://dx.doi.org/10.1021/acsomega.9b03904
ACS Omega 2020, 5, 9702−9706

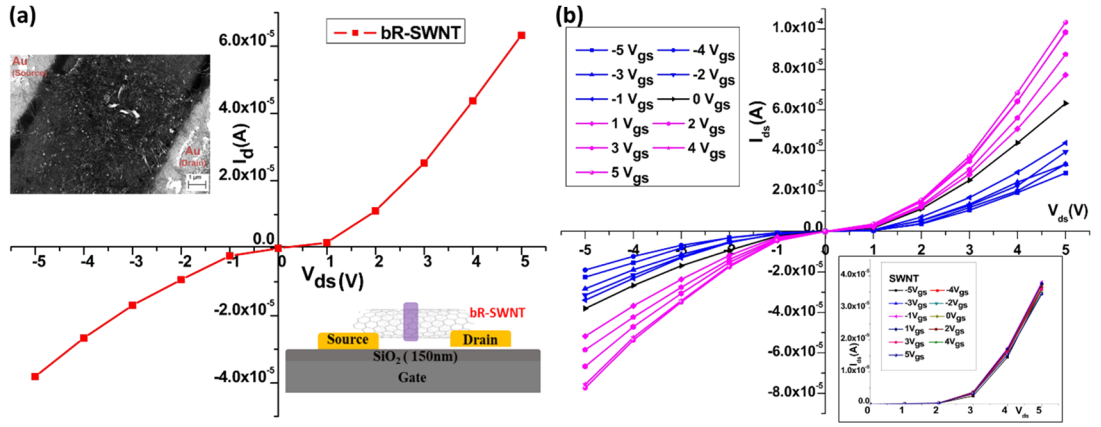

Figure 3. (a) Comparative $I-V$ characteristics of the FET based on SWNTs functionalized with bacteriorhodopsin (bR). A SEM image of the device fabricated is shown as an inset along with the schematic of the FET. (b) $I-V$ characteristics of the fabricated FET based on the functionalized SWNT−bR complex for a range of gate bias applied [−5 V_{gs}, +5 V_{gs}].

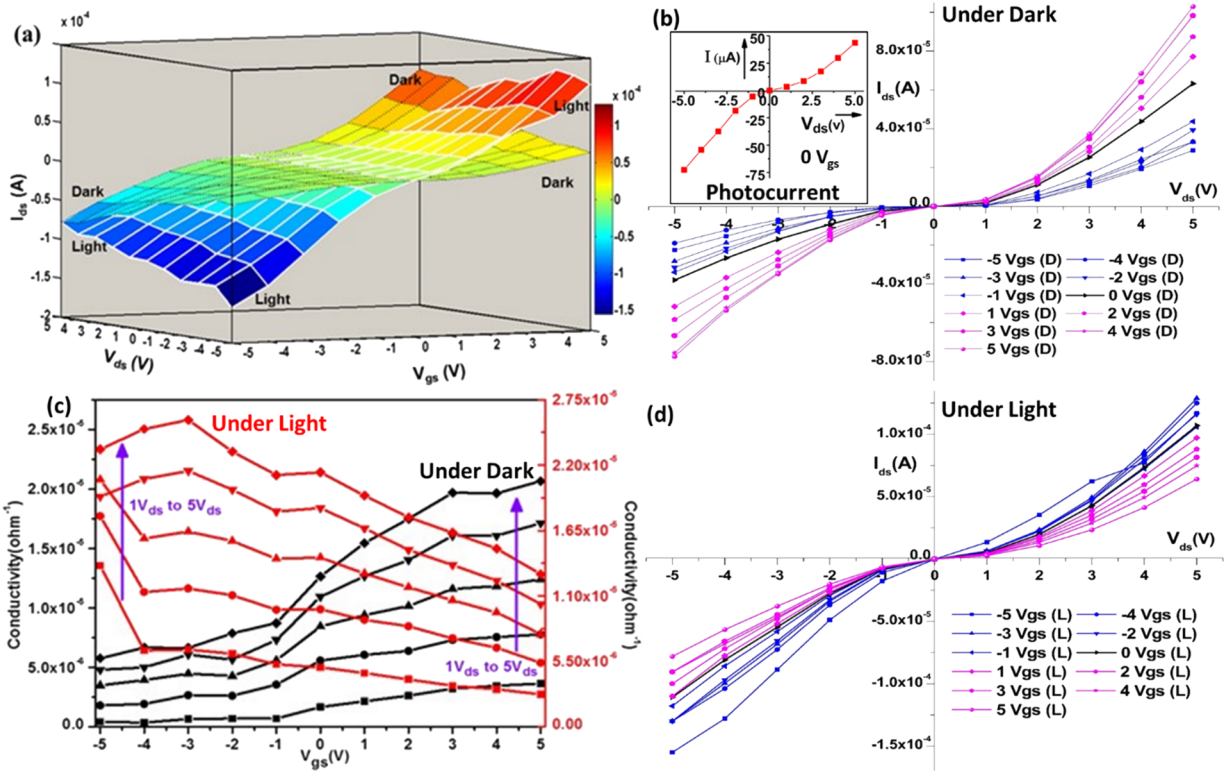

Figure 4. (a) Three-dimensional plot of the current−voltage ($I-V$) response of the device with varying drain−source and gate voltages applied under conditions of dark and light. (b) $I-V$ plot of the bR−SWNT FET at various gate voltages under dark condition (pink for positive gate voltages and blue for negative gate voltages). The inset shows the photocurrent at 0 gate voltages. (c) Plot showing optical doping with the device switching from n-type (black) under dark to p-type under light (red). (d) $I-V$ plot of the bR−SWNT FET at various gate voltages under light condition.

dispersed stable aqueous solution of SWNTs was obtained at the ratio of 1:7.5 (1 part of SWNT with 7.5 parts of PlPEG amine). The measured absorption spectra (UV−vis NIR) of the prepared aqueous solutions do not show any discernible changes in the concentration of SWNTs over weeks. Aqueous solution of 10^{-3} M concentration of the synthesized purple membrane (PM) and dispersed SWNT solution was prepared. Aggregated SWNTs functionalized with the PM were optically aggregated and then separated by the established protocol as reported.[10] The aqueous solution of SWNTs stirred with the purple membrane was illuminated by a broadband mercury lamp for 3 h, and aggregated flocs of functionalized SWNTs were separated from the dispersed supernatant using centrifugation. Separated aggregates of functionalized SWNTs were then drop-casted onto the fabricated device and further characterized using Raman spectroscopy. Figure 1b,c shows SEM images of pristine (top) and that of separated aggregates of SWNT functionalized with bacteriorhodopsin. Bacteriorhodopsin crystals in the purple membrane are expected to be ∼500 nm, whereas pristine SWNTs are ∼1−2 μm in length with diameters varying from 0.7 up to 1.8 nm. HR-SEM images have been taken using a ZEISS system with

https://dx.doi.org/10.1021/acsomega.9b03904
ACS Omega 2020, 5, 9702−9706

backscattering configuration. Images with SWNTs extended out from the matrices of the two-dimensional bacteriorhodopsin protein complex, particularly displaying surface functionalization and a stable hybrid complex required for further fabrication of functional devices.

The hybrid complex of SWNT functionalized with bacteriorhodopsin was further characterized using a Raman spectrometer with a 632 red laser line. The Raman spectra (Figure 2) of the functionalized samples show stable and preferential binding of bR with SWNTs of specific diameters. The RBM of the Raman spectra essentially depends on the diameter of the SWNTs, which may be calculated using the relation $\omega_{RBM} = (\alpha_{RBM}/d) + \alpha_{bundle}$. Here, α_{RBM} and α_{bundle} are constants and d is the diameter of the SWNT corresponding to the RBM peak frequency (ω_{RBM}).[21]

The histogram (Figure 2c) as calculated from the RBM of the Raman spectra (Figure 2a) shows enrichment of specific diameters of SWNTs in the hybrid complex. Discernible changes in the G band of functionalized SWNTs are observed as compared to pure SWNTs. Changes in the G^- band are related to the metallicity of the SWNTs and have been shown to vary with the changes in the electronic properties of the nanotubes. A redshift of ~6 cm^{-1} is observed in SWNTs functionalized with the bR. This redshift in the functional SWNTS can be attributed to strong interaction and electronic doping by the bacteriorhodopsin.[22] Using a similar approach as reported by Rao et al. to estimate electronic doping by corresponding shifts in the Raman peaks, the redshift in our devices indicates doping by an estimated charge density of about $n \approx 3 \times 10^6$ cm^{-2}.

Devices were fabricated using standard lift-off technology and direct laser lithography to pattern metallic pads on a p-type doped silicon wafer (purchased from Semiconductor Wafer, Inc.). Metallic patterns act as a source and drain, whereas a sample holder (chuck) acts as the back gate of the field-effect transistor. The hybrid film of the purple membrane and SWNTs acts as the functional semiconducting channel of the fabricated FET.

Figure 3a (inset) shows the HR-SEM image of the fabricated FET. Devices were electro-optically characterized using an integrated probe station having micromanipulators attached with a dedicated Keithley 4200 SCS semiconductor characterization system. Control $I-V$ measurements of the devices, which were fabricated using pristine SWNTs, do not exhibit any significant gate control (inset, Figure 3b). However, devices functionalized with bR show characteristic n-type semiconducting behavior and significantly enhanced control on current using gate voltages. The observed nonlinear $I-V$ characteristics are attributed to complex electronic transport in the network of functionalized SWNTs,[26] more so as the samples are functionalized with an optically active proton pump like bacteriorhodopsin.[16] The FET shows higher (maximum observed on/off ratio, 8.5) current for positive gate voltages (0 to 5 V) as compared to applied negative voltages (0 to −5 V). The decrease in current is observed with the corresponding increase in applied negative gate voltages (33 μS/m for V_g = 5 V, 9.6 μS/m for V_g = −1 V, and 0.14 μS/m for V_g = −5 V) demonstrating well-controlled electronic gating of the device.

Moreover, under light, optical doping is observed. Figure 4 compares the electronic characteristics of the device under dark and broadband illumination by a mercury lamp. The FET devices based on SWNTs functionalized with bR show n-type characteristics under dark condition, but under broadband illumination from a mercury lamp, FET devices switch to p-type characteristics. Optical doping is observed in the hybrid device due to proton charge transfer from the photoactive proton pump bR to SWNT.[23] The proton transfer mechanism and energy coupling in the bacteriorhodopsin photocycle have been well established; however, a bio−nano hybrid system of semiconducting single-walled carbon nanotubes functionalized with optically active bacteriorhodopsin forms a complex electronic transport network. The following results demonstrate interplay of electronic transport in the complex network of SWNTs and optical proton pumping by the bacteriorhodopsin. Figure 4a demonstrates the $I-V$ characteristics of the functionalized FET under light and dark conditions. The device is "on" for positive gate voltages (0 to 5 V_{gs}) in dark condition and is "on" for negative gate voltages (−5 to 0 V_{gs}) in light condition (Figure 4). An on/off ratio of 8.5 in dark condition and 4.9 in the light condition is observed. The device shows a maximum photocurrent ($I_{Light} - I_{Dark}$) of 40 μA at 5 V_{ds} and 0 V_{gs} with the conductivity of 13.15 μS/m (inset, Figure 4b). Comparing the current between both light and dark conditions, it is seen that current decreases by 60% (5 V_{ds} & 5 V_{gs}) for positive gates and increases by 300% (5 V_{ds} & −5 V_{gs}) for negative gates under the light.

Thus, we observe significant electronic gating of the functionalized FET and excellent optical doping under light and dark conditions. This can be attributed to well-established photocycle and proton transfer properties of bR,[24] thereby affecting electronic conduction through the functionalized SWNT. SWNT FET devices works on the principle of Schottky barriers at the metal semiconductor contact.[25] SWNTs are generally ambipolar, with symmetrical changes in current for both positive and negative gate voltages.[26] However, since electronic transport through the device significantly depends on the Schottky barrier, any modulation in electronic concentration is expected to cause significant changes in the electronic property of the device. Due to considerable changes in the surface charges, functionalization of SWNTs with bacteriorhodopsin is expected to induce band bending, thus affecting the electronic transport of the nanotubes through the Schottky barrier. Switching of the device from n-type to p-type under optical illumination is attributed to optical doping due to proton transfer from optically excited bacteriorhodopsin onto the semiconducting SWNTs. Although further research is in progress to understand the charge transfer and transport mechanism in this hybrid donor−acceptor system, the results confirm optical activation of the proton pump purple membrane with significant charge transfer onto the SWNTs, thereby converting n-type functionalized SWNT FETs into p-type devices. Moreover, optimization of the surface functionalization with better controlled layering and deposition protocols should lead to a higher efficiency, smaller response time, and better on/off ratio of the devices.

CONCLUSIONS

In conclusion, we have shown a stable, optically functional bioelectronic device based on the purple membrane and SWNT complex. Both optical doping and significant optical switching are observed in fabricated FETs. Devices also show considerable photocurrent and electronic gating. The well-controlled electro-optical functionality of the device is due to strong interaction and charge transfer between the 2D optically

https://dx.doi.org/10.1021/acsomega.9b03904
ACS Omega 2020, 5, 9702−9706

active bacteriorhodopsin and electronic single-walled carbon nanotubes, as also affirmed by the Raman spectral analysis. We believe that the results discussed here will be important for diverse biophotonic, bioelectronic, biosensing, and photovoltaic applications. Results shown here may also contribute to realizing functionally reconfigurable biophotonic, electro-optical devices with devices showing a reversible and controlled change in the types of majority carriers, depending on the condition whether the device is under illumination or is in dark. Optical doping, electro-optical switching, and electronic gating, the fact that each of these phenomena reported above is using a bio−nano hybrid complex and realized in the same device, promises potential for widespread application in diverse areas from biological sciences to electronic photonic hybrid sensors and devices.

AUTHOR INFORMATION

Corresponding Author

Harsh Chaturvedi − *Center for Energy, Indian Institute of Technology (IIT), Guwahati, Assam 781039, India;* orcid.org/0000-0002-8319-4589; Phone: +91 361 258 3130; Email: harshc@iitg.ac.in; Fax: +91 361 2690762

Authors

Vikram Bakaraju − *Department of Physics, University of Antwerp, Antwerp 2000, Belgium; G Lab Innovations Pvt. Ltd., Kolkata, West Bengal 700001, India*

E. Senthil Prasad − *Institute of MicrobioTechnology (IMTECH), Chandigarh 160036, India*

Brijesh Meena − *Center for Energy, Indian Institute of Technology (IIT), Guwahati, Assam 781039, India; G Lab Innovations Pvt. Ltd., Kolkata, West Bengal 700001, India*

Complete contact information is available at: https://pubs.acs.org/10.1021/acsomega.9b03904

Notes

The authors declare no competing financial interest.

ACKNOWLEDGMENTS

Authors are deeply indebted to the funding agencies DST (DST/TSG/PT/2012/66) and Nanomission (SR/NM/NS-15/2012) for generous grants and support. Part of the work was done at IISER Pune.

REFERENCES

(1) Bräuchle, C.; Hampp, N.; Oesterhelt, D. Optical applications of bacteriorhodopsin and its mutated variants. *Adv. Mater.* **1991**, *3*, 420−428.

(2) Hampp, N. Bacteriorhodopsin as a photochromic retinal protein for optical memories. *Chem. Rev.* **2000**, *100*, 1755−1776.

(3) Huang, Y.; Wu, S.-T.; Zhao, Y. All-optical switching characteristics in bacteriorhodopsin and its applications in integrated optics. *Opt. Express.* **2004**, *12*, 895−906.

(4) Borghetti, J.; Derycke, V.; Lenfant, S.; Chenevier, P.; Filoramo, A.; Goffman, M.; Vuillaume, D.; Bourgoin, J.-P. Optoelectronic switch and memory devices based on polymer-functionalized carbon nanotube transistors. *Adv. Mater.* **2006**, *18*, 2535−2540.

(5) Staii, C.; Johnson, A. T.; Chen, M.; Gelperin, A. DNA-decorated carbon nanotubes for chemical sensing. *Nano Lett.* **2005**, *5*, 1774−1778.

(6) Shim, M.; Shi Kam, N. W.; Chen, R. J.; Li, Y.; Dai, H. Functionalization of carbon nanotubes for biocompatibility and biomolecular recognition. *Nano lett.* **2002**, *2*, 285−288.

(7) Keren, K.; Berman, R. S.; Buchstab, E.; Sivan, U.; Braun, E. DNA-templated carbon nanotube field-effect transistor. *Science* **2003**, *302*, 1380−1382.

(8) Singh, R.; Pantarotto, D.; McCarthy, D.; Chaloin, O.; Hoebeke, J.; Partidos, C. D.; Briand, J.-P.; Prato, M.; Bianco, A.; Kostarelos, K. Binding and condensation of plasmid DNA onto functionalized carbon nanotubes: toward the construction of nanotube-based gene delivery vectors. *J. Am. Chem. Soc.* **2005**, *127*, 4388−4396.

(9) Katz, E.; Willner, I. Biomolecule-functionalized carbon nanotubes: applications in nanobioelectronics. *ChemPhysChem* **2004**, *5*, 1084−1104.

(10) Shamra, A.; Prasad, E. S.; Chaturvedi, H. Photon induced separation of bio-nano hybrid complex based on carbon nanotubes and optically active bacteriorhodopsin. *Opt. Mater. Express* **2016**, *6*, 986−992.

(11) Guldi, D. M.; Rahman, G. M. A.; Zerbetto, F.; Prato, M. Carbon nanotubes in electron donor− acceptor nanocomposites. *Acc. Chem. Res.* **2005**, *38*, 871−878.

(12) Barone, P. W.; Baik, S.; Heller, D. A.; Strano, M. S. Near-infrared optical sensors based on single-walled carbon nanotubes. *Nat. Mater.* **2005**, *4*, 86−92.

(13) Wang, J. Carbon-nanotube based electrochemical biosensors: A review. *Electroanalysis* **2005**, *17*, 7−14.

(14) Jin, Y.; Honig, T.; Ron, I.; Friedman, N.; Sheves, M.; Cahen, D. Bacteriorhodopsin as an electronic conduction medium for biomolecular electronics. *Chem. Soc. Rev.* **2008**, *37*, 2422−2432.

(15) Lu, Z.; Wang, J.; Xiang, X.; Li, R.; Qiao, Y.; Li, C. M. Integration of bacteriorhodopsin with upconversion nanoparticles for NIR-triggered photoelectrical response. *Chem. Commun.* **2015**, *51*, 6373−6376.

(16) Lozier, R. H.; Bogomolni, R. A.; Stoeckenius, W. Bacteriorhodopsin: a light-driven proton pump in Halobacterium Halobium. *Biophys. J.* **1975**, *15*, 955−962.

(17) Xu, J.; Bhattacharya, P.; Váró, G. Monolithically integrated bacteriorhodopsin/semiconductor opto-electronic integrated circuit for a bio-photoreceiver. *Biosens. Bioelectron.* **2004**, *19*, 885−892.

(18) Wang, W. W.; Knopf, G. K.; Bassi, A. S. Photoelectric properties of a detector based on dried bacteriorhodopsin film. *Biosens. Bioelectron.* **2006**, *21*, 1309−1319.

(19) Vaisman, L.; Wagner, H. D.; Marom, G. The role of surfactants in dispersion of carbon nanotubes. *Adv. Colloid Interface Sci.* **2006**, *128-130*, 37−46.

(20) Liu, Z.; Tabakman, S. M.; Chen, Z.; Dai, H. Preparation of carbon nanotube bioconjugates for biomedical applications. *Nat. Protoc.* **2009**, *4*, 1372.

(21) Bachilo, S. M.; Strano, M. S.; Kittrell, C.; Hauge, R. H.; Smalley, R. E.; Weisman, R. B. Structure-assigned optical spectra of single-walled carbon nanotubes. *Science* **2002**, *298*, 2361−2366.

(22) Rao, C. N. R.; Voggu, R. Charge-transfer with graphene and nanotubes. *Mater. Today* **2010**, *13*, 34−40.

(23) Inoue, K.; Ito, S.; Kato, Y.; Nomura, Y.; Shibata, M.; Uchihashi, T.; Tsunoda, S. P.; Kandori, H. A natural light-driven inward proton pump. *Nat. Commun.* **2016**, *7*, 1−10.

(24) Lanyi, J. K. Proton transfers in the bacteriorhodopsin photocycle. *Biochim. Biophys. Acta, Bioenerg.* **2006**, *1757*, 1012−1018.

(25) Svensson, J.; Campbell, E. E. B. Schottky barriers in carbon nanotube-metal contacts. *J. Appl. Phys.* **2011**, *110*, 111101.

(26) Bisri, S. Z.; Derenskyi, V.; Gomulya, W.; Salazar-Rios, J. M.; Fritsch, M.; Fröhlich, N.; Jung, S.; Allard, S.; Scherf, U.; Loi, M. A. Anomalous Carrier Transport in Ambipolar Field-Effect Transistor of Large Diameter Single-Walled Carbon Nanotube Network. *Adv. Electron. Mater.* **2016**, 1500222.